High-performance large-area organic perovskite devices for lighting, energy and pervasive communications

Recent results on metal halide perovskites and their interfaces

March 14th 2022

Boubacar Traore, Claudio Quarti, Junke Jiang, Laurent Pedesseau, Yorgos Volonakis, Mikael Kepenekian, Jacky Even and Claudine Katan
claudine.katan@cnrs.fr

Objectives | Advance perovskite technologies

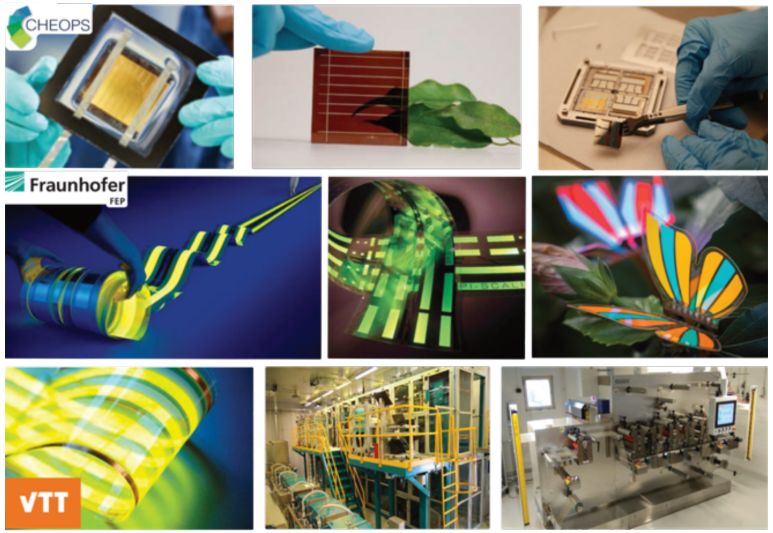

Key technical objectives

1. Development of organic-inorganic perovskite materials for lighting (PeLED) and photovoltaic (PePV) devices
2. Demonstration of large-area PeLED and PePV on flexible substrates
3. Materials & processing advances supported by the development of effective (laser-based) characterization tools based on AFM-IR and Raman spectroscopy
4. Demonstration of environmentally stable devices
5. Integration of PeroCUBE devices into wearables/smart devices & LiFi technologies

Introduction | perovskite structures

$BO_6 – MX_6$ octahedra

Perovskite network =
maintain
at least some **corner-sharing**

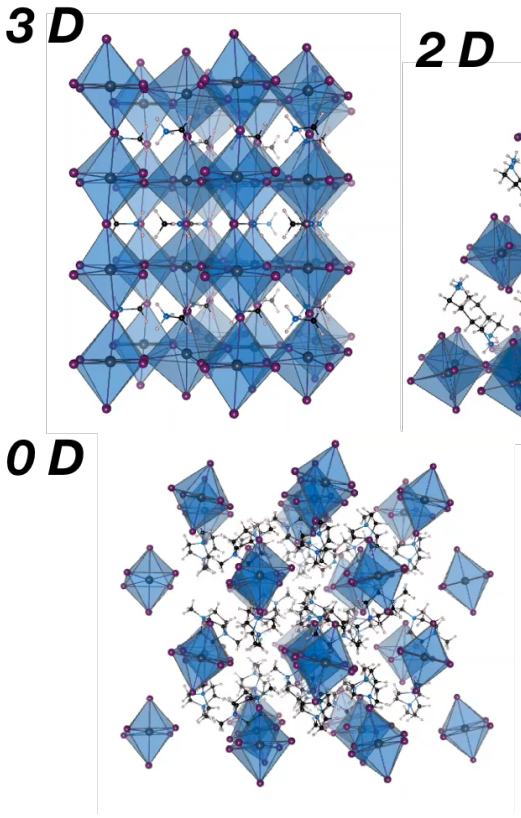

Mixed network =
perovskitoids

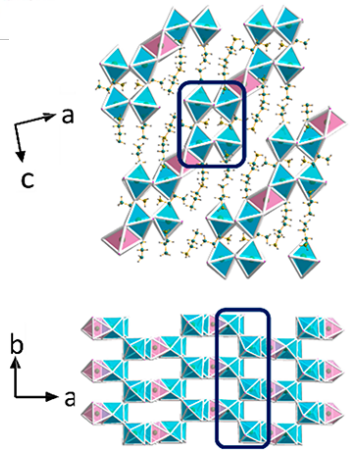

N. Mercier, CrystEngComm, 11, 720 (2009); B. Saparov, Chem. Rev. 116, 4558 (016); C. C. Stoumpos, Inorg. Chem. 56, 56 (2017); Chem. Rev. perovskite Special Issue 2019, 119

Introduction | perovskite structures

AMX_3 3D perovskite

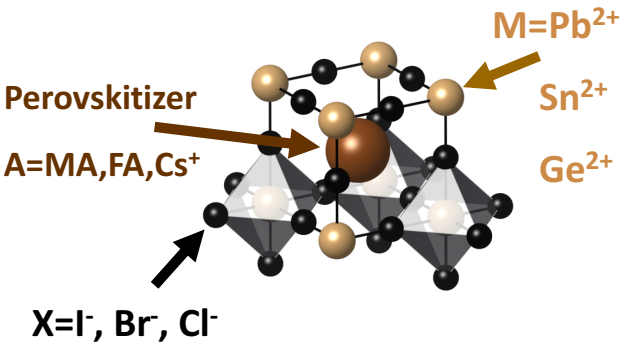

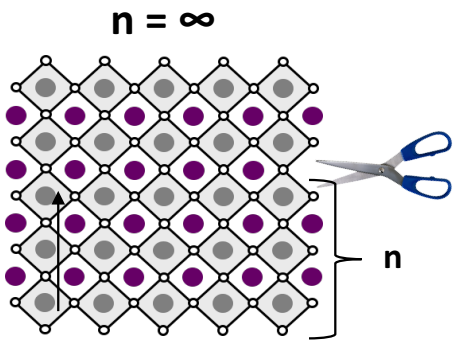

<100>

+ **A'** = "larger" organic cation / dication

+ slicing

+ **A** = "larger" molecule

A'_2MX_4 2D and multi-layered perovskites[1]

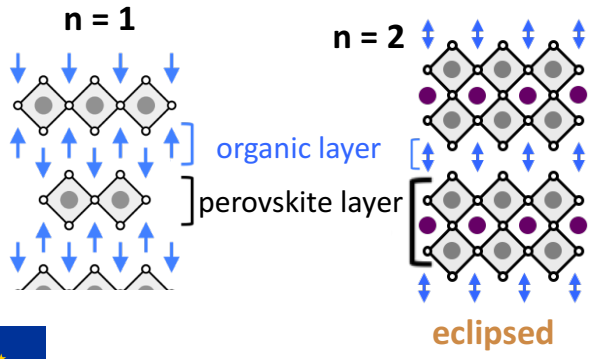

hollow[2]/deficient[3]

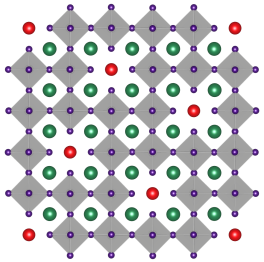

new 3D & 2D perovskitoids[4]

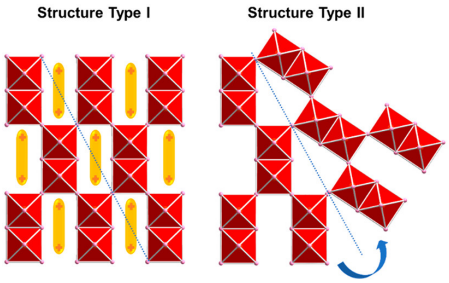

[1] C. Katan, Chem. Rev. 119, 3140 (2019); [2] M. L. Aubrey, Nature 597, 355 (2021); [3] X. Li, JACS, 142, 11486 (2020); [4] I. Spanopoulos, JACS 143, 7069(2017);[5] A. Leblanc, Angew. Chem. Int. Ed 56, 16067, [4] X. Li, JACS, 144, 3902 (2022)

Introduction | main challenges

- improve device performances, including on large and flexible substrates
- solve environmental hazards
  - toxicity of materials
  - during the manufacturing processes (e.g. solvants)
- several issues related to **stability**:
  - of the material
    - perovskite phase instability
    - degradation in ambient conditions
    - degradation under operational conditions
    - degradation related to interfacial materials (ETL/HTL…)
  - of device performances
    - over time
    - under operational conditions (e.g. light)

Introduction | main challenges

- improve device performances and stability:
  - complex alloys

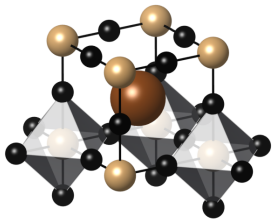

SOLAR CELLS *Science 2016*

Incorporation of rubidium cations into perovskite solar cells improves photovoltaic performance

Michael Saliba,[1]*† Taisuke Matsui,[1,2]† Konrad Domanski,[1]† Ji-Youn Seo,[1] Amita Ummadisingu,[1] Shaik M. Zakeeruddin,[1] Juan-Pablo Correa-Baena,[3] Wolfgang R. Tress,[1] Antonio Abate,[1] Anders Hagfeldt,[3] Michael Grätzel[1]*

SOLAR CELLS

A mixed-cation lead mixed-halide perovskite absorber for tandem solar cells *Science 2016*

David P. McMeekin,[1] Golnaz Sadoughi,[1] Waqaas Rehman,[1] Giles E. Eperon,[1] Michael Saliba,[1] Maximilian T. Hörantner,[1] Amir Haghighirad,[1] Nobuya Sakai,[1] Lars Korte,[2] Bernd Rech,[2] Michael B. Johnston,[1] Laura M. Herz,[1] Henry J. Snaith[1]*

- defect passivation / additives

SOLAR CELLS *Science 2019*

Carrier lifetimes of >1 µs in Sn-Pb perovskites enable efficient all-perovskite tandem solar cells

Jinhui Tong[1,2]*, Zhaoning Song[3]*, Dong Hoe Kim[1]*†, Xihan Chen[1], Cong Chen[3], Axel F. Palmstrom[1], Paul F. Ndione[1], Matthew O. Reese[1], Sean P. Dunfield[1,2,4], Obadiah G. Reid[1,2], Jun Liu[1], Fei Zhang[1], Steven P. Harvey[1], Zhen Li[1], Steven T. Christensen[1], Glenn Teeter[1], Dewei Zhao[3], Mowafak M. Al-Jassim[1], Maikel F. A. M. van Hest[1], Matthew C. Beard[1], Sean E. Shaheen[2,5], Joseph J. Berry[1]‡, Yanfa Yan[3]‡, Kai Zhu[1]‡

Ligand-engineered bandgap stability in mixed-halide perovskite LEDs *Nature 2021*

https://doi.org/10.1038/s41586-021-03217-8
Received: 3 July 2020
Accepted: 11 January 2021
Published online: 3 March 2021

Yasser Hassan[1,15]✉, Jong Hyun Park[2,15], Michael L. Crawford[3], Aditya Sadhanala[1,4,5], Jeongjae Lee[6], James C. Sadighian[3], Edoardo Mosconi[7], Ravichandran Shivanna[5], Eros Radicchi[7,8], Mingyu Jeong[9], Changduk Yang[9], Hyosung Choi[10], Sung Heum Park[11], Myoung Hoon Song[2], Filippo De Angelis[7,8,12], Cathy Y. Wong[3,13,14]✉, Richard H. Friend[5], Bo Ram Lee[11]✉ & Henry J. Snaith[1]✉

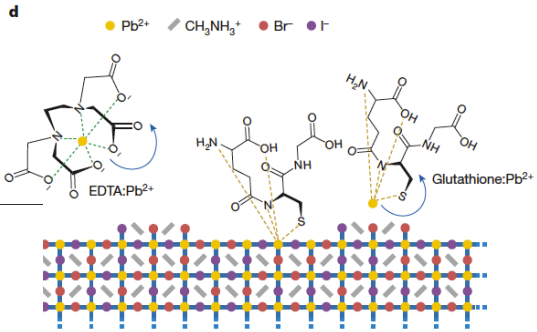

[1] M. Saliba, Science, 354, 206 (2016); [2] D. McMeekin, Science, 351, 151 (2016),[3] J. Tong, Science, 364, 475 (2019); [4] Y. Hassan, Nature, 591, 72 (2021)

Introduction | main challenges

- improve device performances and stability:
  - complex alloys **& 2D/3D mixtures**

Phenylalkylamine Passivation of Organolead Halide Perovskites Enabling High-Efficiency and Air-Stable Photovoltaic Cells *Adv. Mater. 2016*

*Feng Wang, Wei Geng, Yang Zhou, Hong-Hua Fang, Chuan-Jia Tong, Maria Antonietta Loi, Li-Min Liu, and Ni Zhao**

- additives/interface

DMSO 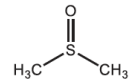

carbohydrazine 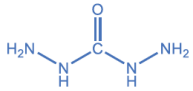

SOLAR CELLS

Stabilizing perovskite-substrate interfaces for high-performance perovskite modules *Science 2021*

Shangshang Chen, Xuezeng Dai, Shuang Xu, Haoyang Jiao, Liang Zhao, Jinsong Huang*

mini-modules with PCEs of 19.3 and 19.2%, aperture areas of 18 and 50 cm^2

Efficient ambient-air-stable solar cells with 2D–3D heterostructured butylammonium-caesium-formamidinium lead halide perovskites

Zhiping Wang, Qianqian Lin, Francis P. Chmiel, Nobuya Sakai, Laura M. Herz and Henry J. Snaith*

Nature Energy 2017

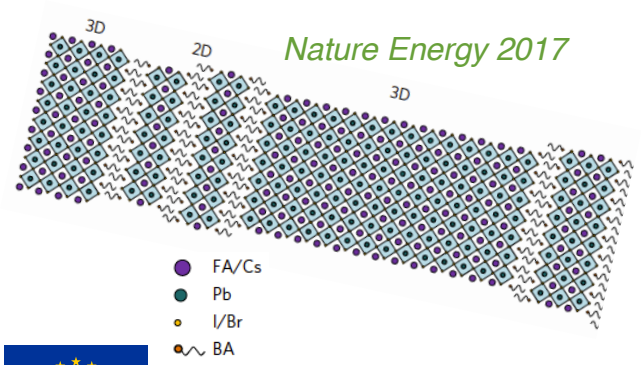

Damp heat-stable perovskite solar cells with tailored-dimensionality 2D/3D heterojunctions *Science 2022*

Randi Azmi[1], Esma Ugur[1], Akmaral Seitkhan[1], Faisal Aljamaan[1], Anand S. Subbiah[1], Jiang Liu[1], George T. Harrison[1], Mohamad I. Nugraha[1], Mathan K. Eswaran[1], Maxime Babics[1], Yuan Chen[2], Fuzong Xu[1], Thomas G. Allen[1], Atteq ur Rehman[1], Chien-Lung Wang[2], Thomas D. Anthopoulos[1], Udo Schwingenschlögl[1], Michele De Bastiani[1], Erkan Aydin[1], Stefaan De Wolf[1]*

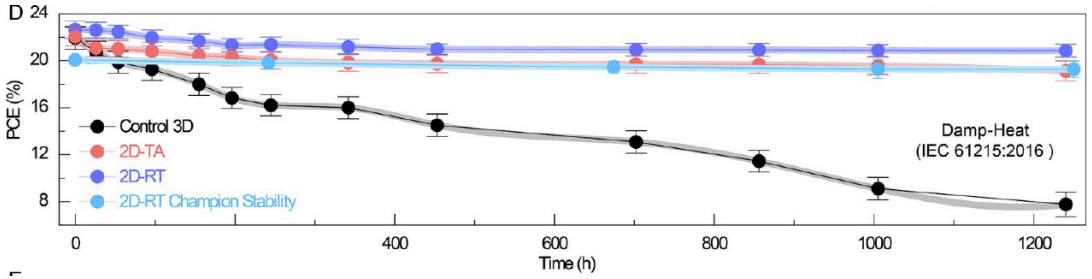

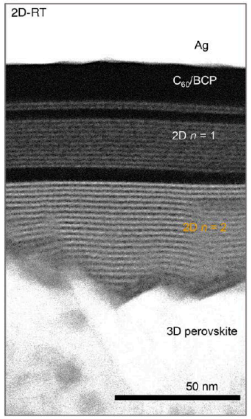

HR-STEM

[1] J. Chen, Science 373, 902 (2021); [2] P. Schulz, Chem. Rev. 119, 3379 (2019); [3] F. Wang, Adv. Mater. 28, 9986 (2016); [4] Z. Wang, Nature Energy, 2, 17135 (2017); [5] R. Azmi, Science (2022), DOI: 10.1126/science.abm5784;

Introduction | open questions

- impact of additional species on optoelectronic properties
  - of perovskite material?
  - of device?
    - working device: band alignment is crucial!
    - strain/dipole - surface/interfaces

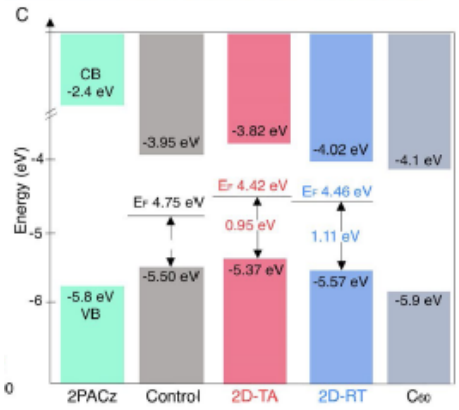

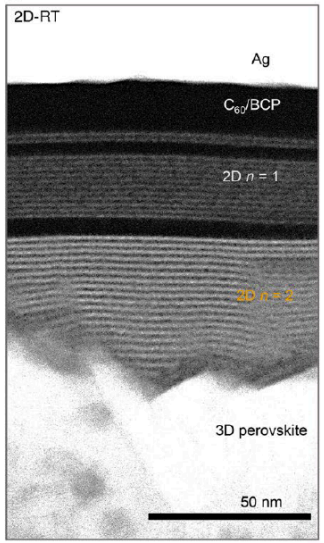

- how can we simulate such large/complex structures and heterostructures
  - affording a microscopic understanding
  - capture the disorder/dynamics/alloying
  - treat ”quantitatively” energetics: pb of costly many-body large/complex structures

[1] R. Azmi, Science 2022, DOI: 10.1126/science.abm5784;

Outline | short summary

- lattice mismatch in multi-layered perovskites
- treatment of complex heterostructures at the first-principles level: DFT within **SIESTA**
  - capturing stochastic dynamics & alloying in a static picture: “pseudo-atoms”
  - *conventions/definitions*
  - revisiting DFT-1/2 for 3D and 2D
- impact of chemical tuning on energetics:
  - effect of lattice strain
  - relation between surface dipole and energetics
    - methodology
    - surface termination
    - surface passivation: empirical rules
    - heterostructures: additivity
- wrap up and brief outlook

Introduction | perovskite structures

multi-layered perovskites and 2D/3D heterostructures[1]

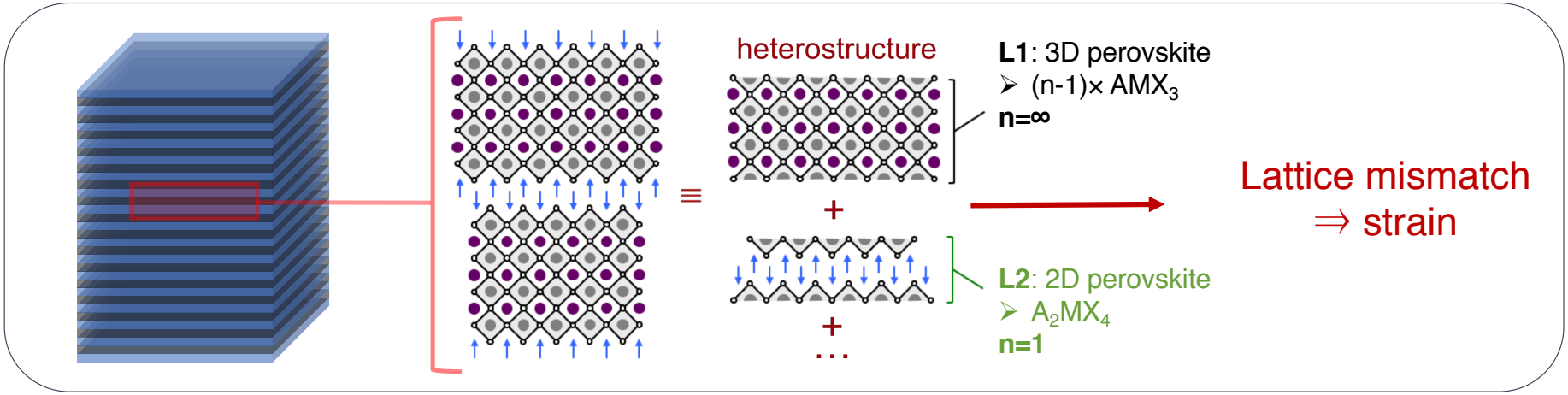

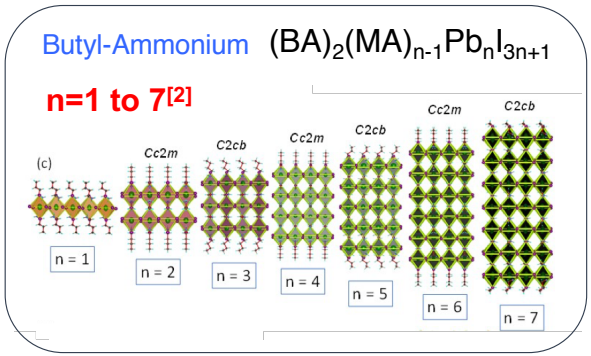

improper flexoelastic model

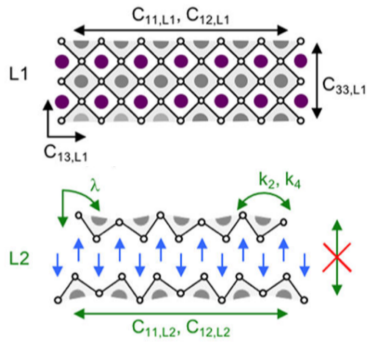

computed

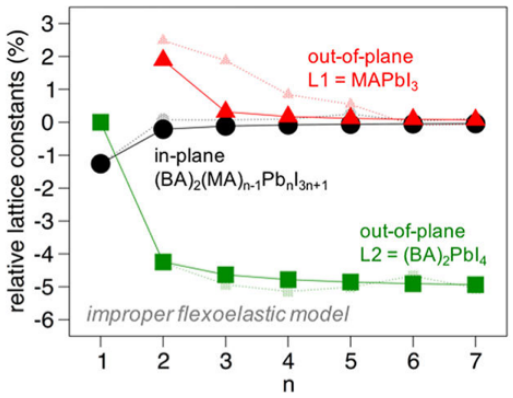

[1] M. Kepenekian, Nano Lett. 18, 5603 (2018); [2] Soe et al. PNAS 116, 58 (2019)

Results | mimic stochastic dynamics/alloying

- Stochastic disorder of the A-site cation

$FAPbI_3$

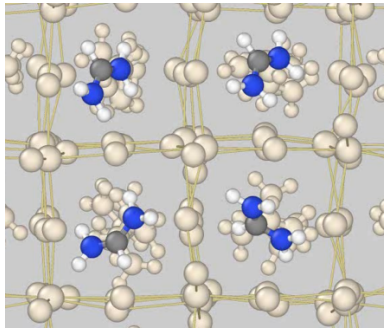

	exp	
	latt. const. (Å)	Mismatch
ref. $FAPbI_3$	6.362	-
n=1	6.212	-2.4%
n=2	6.295	-1.1%
n=3	6.295	-1.1%
n=4	6.296	-1.0%

	relaxed (C09+DF2)	
	latt. const. (Å)	mismatch
ref. FA^*PbI_3	6.306	
n=1	6.134	-2.7%
n=2	6.174	-2.1%
n=3	6.206	-1.6%
n=4	6.217	-1.4%

FA*= Cs

[1] B. Traore, to be published;

Results | mimic stochastic dynamics/alloying

- Stochastic disorder of the A-site cation

$FAPbI_3$

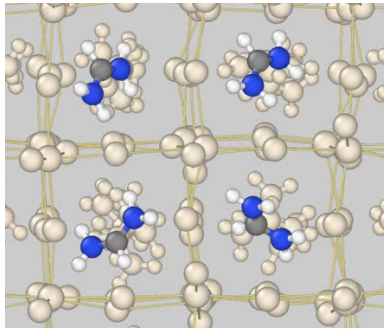

	exp	
	latt. const. (Å)	Mismatch
ref. $FAPbI_3$	6.362	-
psc-$CsPbI_3$	6.201	-2.5%
n=1	6.212	-2.4%
n=2	6.295	-1.1%
n=3	6.295	-1.1%
n=4	6.296	-1.0%

	relaxed (C09+DF2)	
	latt. const. (Å)	mismatch
ref. FA^*PbI_3	6.306	
psc-Cs^*PbI_3	6.164	-2.3%
n=1	6.134	-2.7%
n=2	6.174	-2.1%
n=3	6.206	-1.6%
n=4	6.217	-1.4%

FA*= Cs

Cs*= Na

- alloying: *virtual crystal approximation*[2]

$(FA_xCs_{1-x})PbI_3$

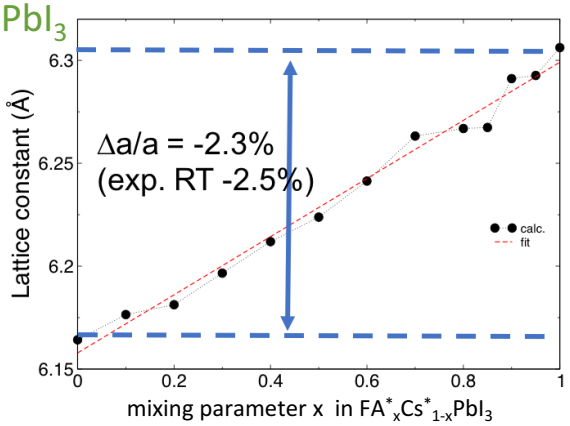

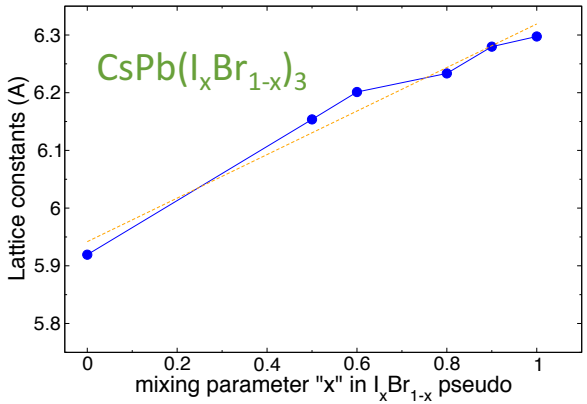

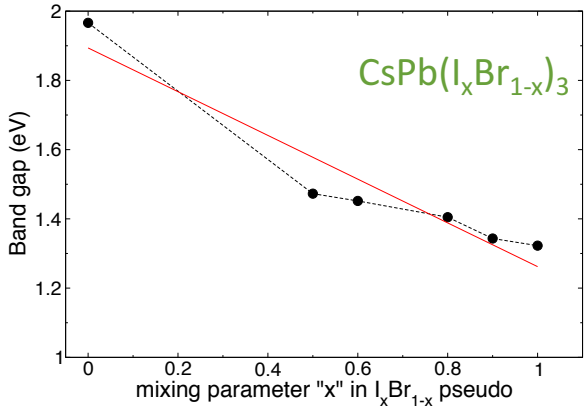

Vegard's law ~well reproduced

[1] B. Traore, to be published; [2] L. Bellaiche, PRB 61, 7877 (2000)

Introduction | convention and definition

- Positive dipole

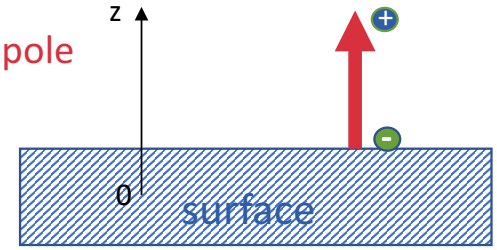

[1] A. Kahn, Mater. Horiz. 3, 7 (2016)

Introduction | convention and definition

- Positive dipole

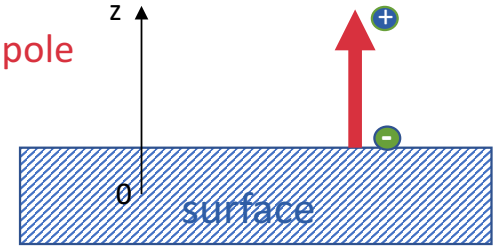

- Valence band energy and Work function

DFT

0 K
undoped
non defective

$E_v^{abs} = -WF$

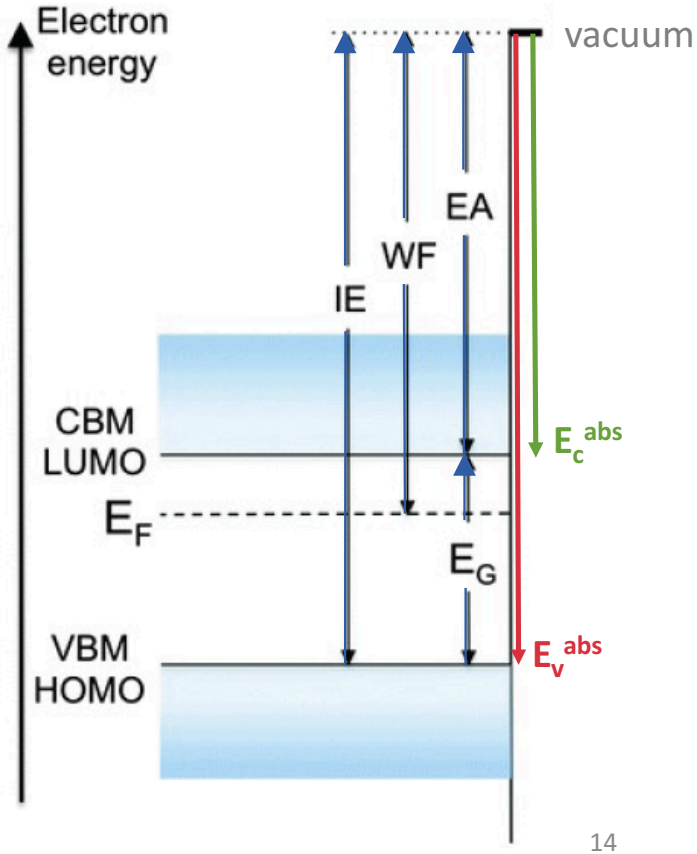

[1] A. Kahn, Mater. Horiz. 3, 7 (2016)

Introduction | convention and definition

- Positive dipole

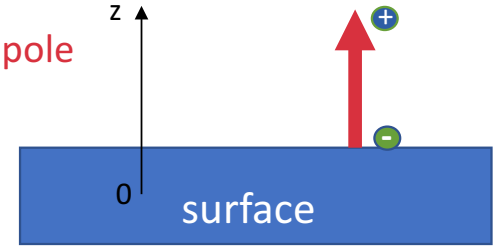

- Energetics: from Hartree potential[1,2]

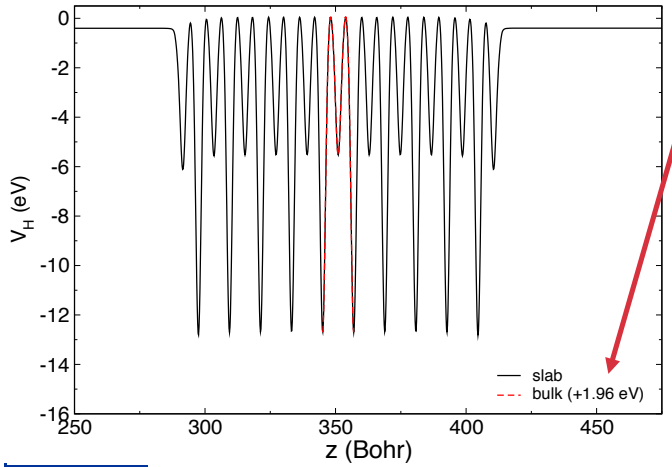

ΔVH = Potential shift to align the bulk VBM to the slab

$E_v^{abs} = VBM_{bulk} + \Delta VH + \Delta V_{vacuum}$

$E_c^{abs} = E_v^{abs} + E_G$

DFT

0 K
undoped
non defective

E_v^{abs} = -WF

- Valence band energy and Work function

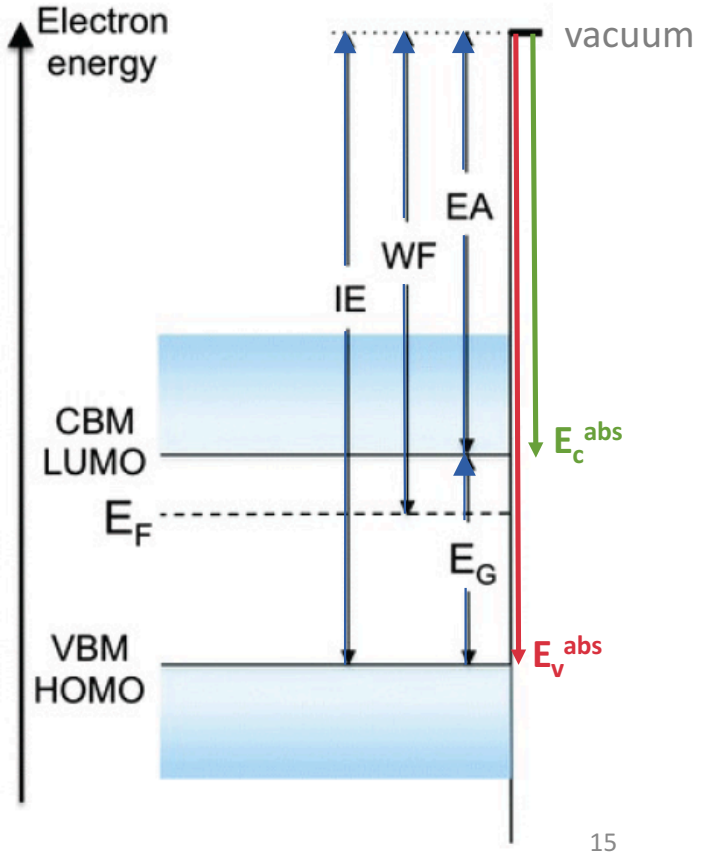

[1] A. Kahn, Mater. Horiz. 3, 7 (2016)

[1] L. Kleinman, PRB 24, 7412 (1980); [2] C. G. van de Walle, PRB 35, 8154 (1987)

Results | towards quantitative band gaps at low cost

DFT-1/2

1. slater half occupation scheme: self-energy that corrects band gaps
2. needs a priori knowledge of VBM atomic orbitals
3. cost similar to GGA

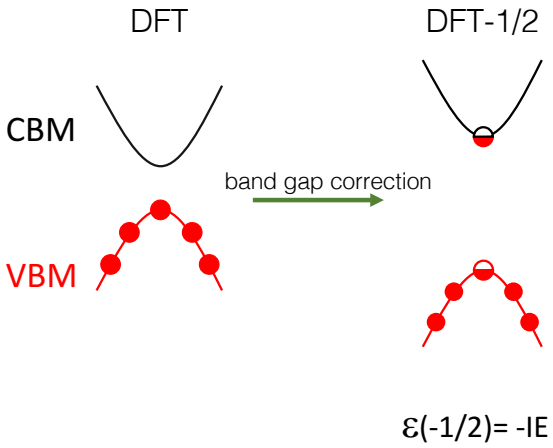

$\varepsilon(-1/2) = -IE$

[1] S. Tao, Scientific report, 7, 14386 (2017)

Results | towards quantitative band gaps at low cost

DFT-1/2

1. slater half occupation scheme: self-energy that corrects band gaps
2. needs a priori knowledge of VBM atomic orbitals
3. cost similar to GGA

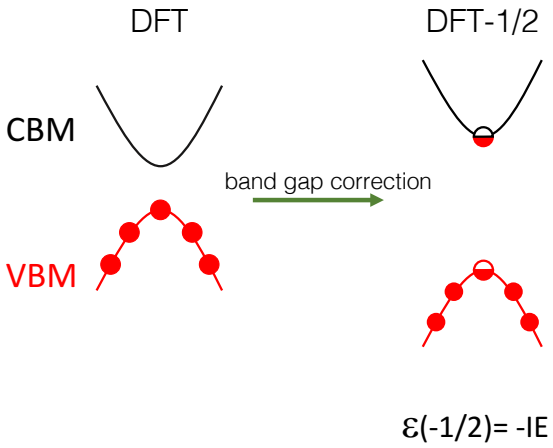

$\varepsilon(-1/2) = -IE$

- revisited[1] for 3D AMX_3 perovskites
  - -1/2 e^- : I *5p* an Pb *6s + optimization of* r_{cut}
  - 12 compositions/phases

gap (eV)	PBE[2]	DFT-1/2[2]	ppTB-mBJ[3]	Exp
$MAPbI_3$ (pnma)	0.64	1.69	1. 64	1.65[4]
MAPE(%)	69	8	6	reference

reduced effective masse μ (m_0)	PBE[2]	DFT-1/2[2]	ppTB-mBJ[3]	Exp
$MAPbI_3$ (pnma) [010] – [101]	0.06-0.08	0.14-0.16	0.17-0.20	0.12[5] 0.15[6]
MAPE(%)	50	20	47	reference

[1] S. Tao, Scientific report, 7, 14386 (2017)
[2] B. Traore, PRM, 6, 014604 (2022); [3] B. Traore, PRB, 99, 035139 (2019);
[4] C. Quarti, EES 9, 155 (2016); [5]M. Hirasawa, Physica B Condens. Matter 201, 427 (1994); [6] K. Tanaka, Solid State Commun. 127, 619 (2003);

Results | towards quantitative band gaps at low cost

DFT-1/2

1. slater half occupation scheme: self-energy that corrects band gaps
2. needs a priori knowledge of VBM atomic orbitals
3. cost similar to GGA

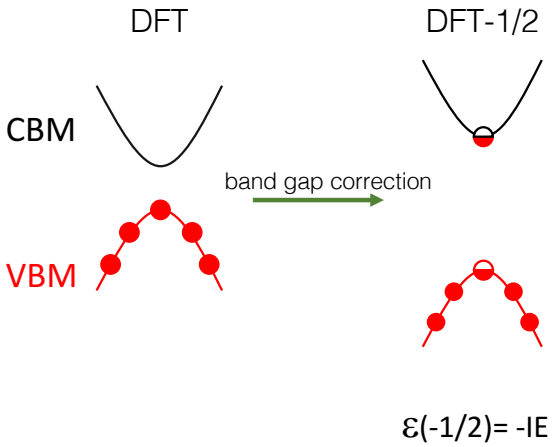

- what about 2D A_2MX_4 perovskites
  - same -1/2 e^- : I *5p* an Pb *6s + same* r_{cut}
  - 30 compositions

gap (eV) / μ (m_0)	PBE[1]	DFT-1/2[1]		Exp
$BA_2MA_{n-1}Pb_nI_{3+1}$				
n=1	1.28 / *0.10*	2.20 / *0.16*		2.80[3] / *0.22*[4]
n=2	0.87 / *0.08*	1.82 / *0.14*		2.44[3] / *0.22*[4]
n=3	0.64 / *0.06*	1.65 / *0.12*		2.26[3] / *0.20*[4]
n=4	0.64 / *0.06*	1.67 / *0.12*		2.15[3] / *0.20*[4]
n=5	0.39 / *0.07*	1.36 / *0.12*		2.08[3] / *0.19*[4]
MAPE(%)	62 / -	19 / -		reference

- band gap n=4,5 < 3D! needs improvements

[1] B. Traore, PRM, 6, 014604 (2022); [2C. Quarti, J. Phys. Mater. 3 042001 (2020); 355, 1288 (2017) [3] J.-C. Blancon, Science 355, 1288 (2017); [4] J.-C. Blancon, Nat. Comm. 9, 2254 (2018)

Results | towards quantitative band gaps at low cost

DFT-1/2

1. slater half occupation scheme: self-energy that corrects band gaps
2. needs a priori knowledge of VBM atomic orbitals
3. cost similar to GGA

- Symmetry analysis

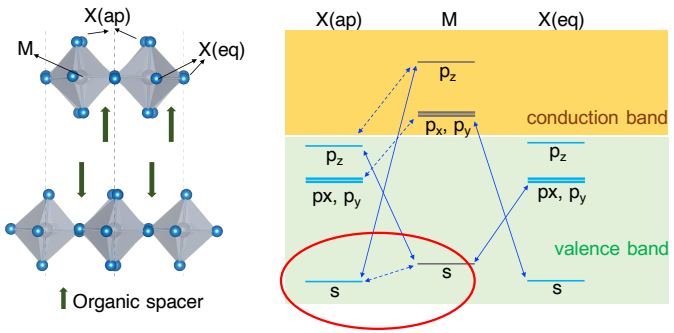

- what about 2D A_2MX_4 perovskites
  - same -1/2 e- : I *5p* an Pb *6s* *+ -1/4 e- I 5s* *+ optimization* r_{cut}
  - 30 compositions

gap (eV) / μ (m_0)	PBE[1]	DFT-1/2[1]	xs-DFT-1/2[1]	Exp
$BA_2MA_{n-1}Pb_nI_{3+1}$				
n=1	1.28 / *0.10*	2.20 / *0.16*	2.84 / *0.18*	2.80[3] / *0.22*[4]
n=2	0.87 / *0.08*	1.82 / *0.14*	2.45 / *0.17*	2.44[3] / *0.22*[4]
n=3	0.64 / *0.06*	1.65 / *0.12*	2.29 / *0.14*	2.26[3] / *0.20*[4]
n=4	0.64 / *0.06*	1.67 / *0.12*	2.32 / *0.14*	2.15[3] / *0.20*[4]
n=5	0.39 / *0.07*	1.36 / *0.12*	2.01/ *0.14*	2.08[3] / *0.19*[4]
MAPE(%)	62 / -	19 / -	12/-	reference

- improves both band gap and in-plane reduced mass

[1] B. Traore, PRM, 6, 014604 (2022); [2] C. Quarti, J. Phys. Mater. 3 042001 (2020); 355, 1288 (2017) [3] J.-C. Blancon, Science 355, 1288 (2017); [4] J.-C. Blancon, Nat. Comm. 9, 2254 (2018)

Results | DFT-1/2 for the energetics

- what about energetics ?

3D slabs

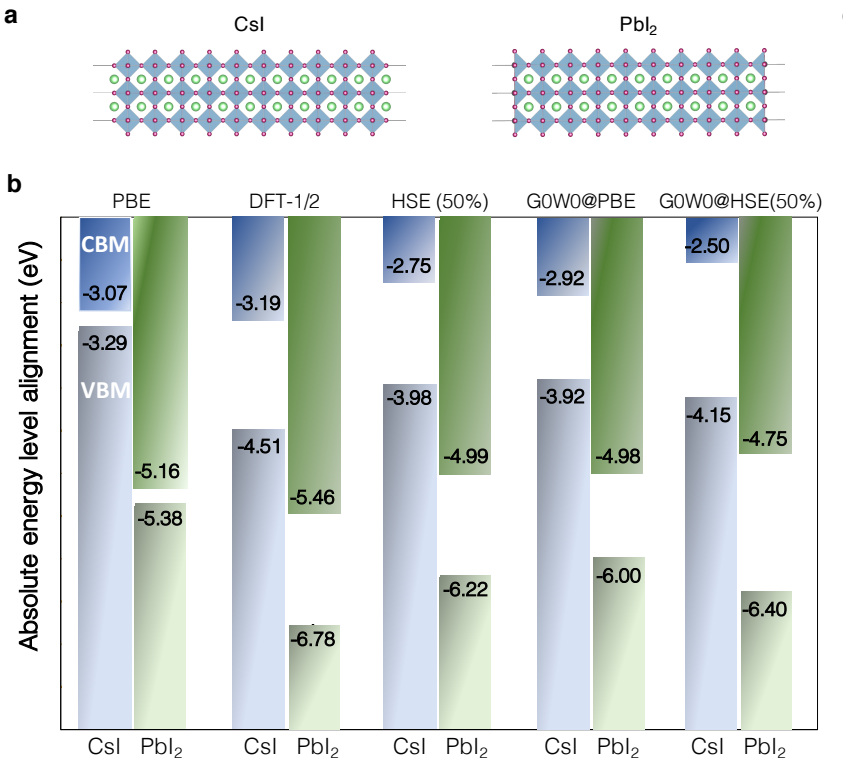

	experimental IE (eV)
$CsPbI_3$[2]	6.25±0.1

Selina Olthof APL Mater. **4**, 091502 (2016)

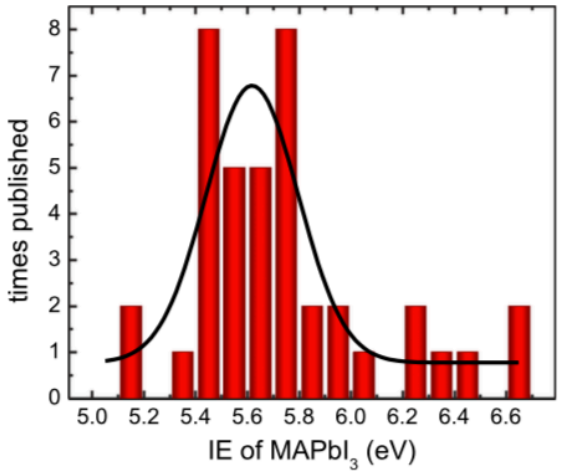

[1] B. Traore, PRM, 6, 014604 (2022); [2] S. Tao, Nat. Comm. 10, 2560 (2019)

Results | DFT-1/2 for the energetics

- what about energetics ?

3D slabs

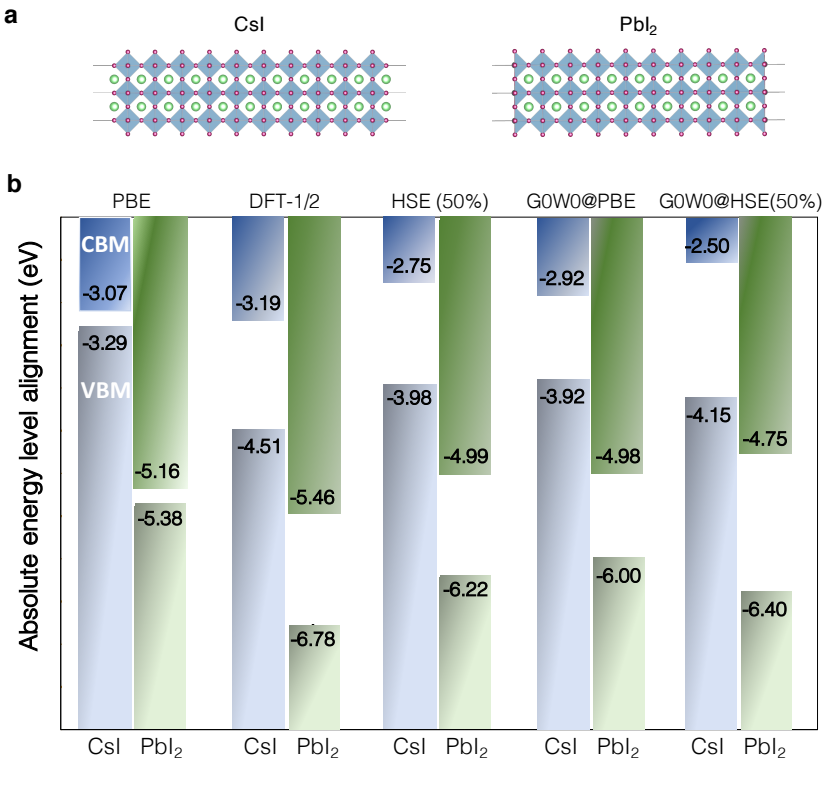

2D slabs

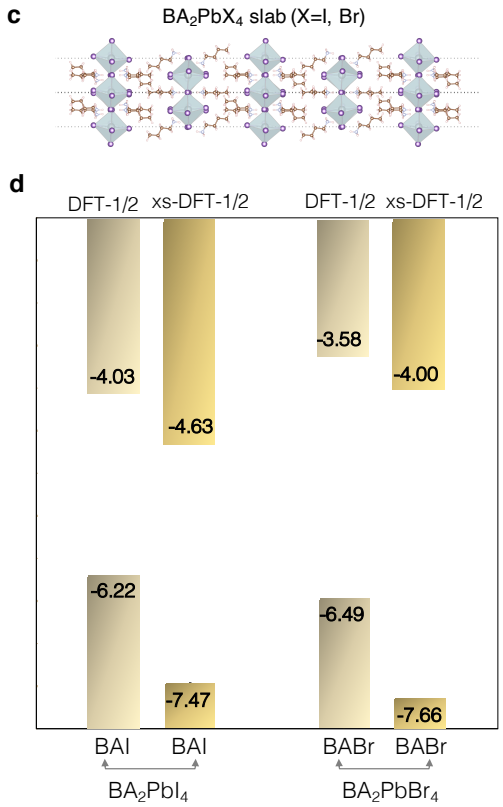

	experimental IE (eV)
$CsPbI_3$[2]	6.25±0.1
BA_2PbI_3[3]	5.8
BA_2PbBr_3[3]	6.5

Take home message

1. DFT-1/2 improves band gaps
2. DFT-1/2 improves effective masses
3. symmetry helps to tune relevant orbitals
4. xs-DFT-1/2 leads to an issue with absolute energetics
5. need for more experimental data on energetics and effective masses, especially for 2D
6. organic still challenging

[1] B. Traore, PRM, 6, 014604 (2022); [2] S. Tao, Nat. Comm. 10, 2560 (2019) [3] S. Silver, Adv. Energy Mater. 1703468 (2018)

results | Effect of lattice strain on energy levels

- model structure : cubic $CsPbI_3$ slab
- CsI terminated

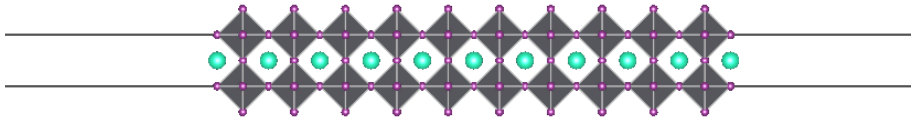

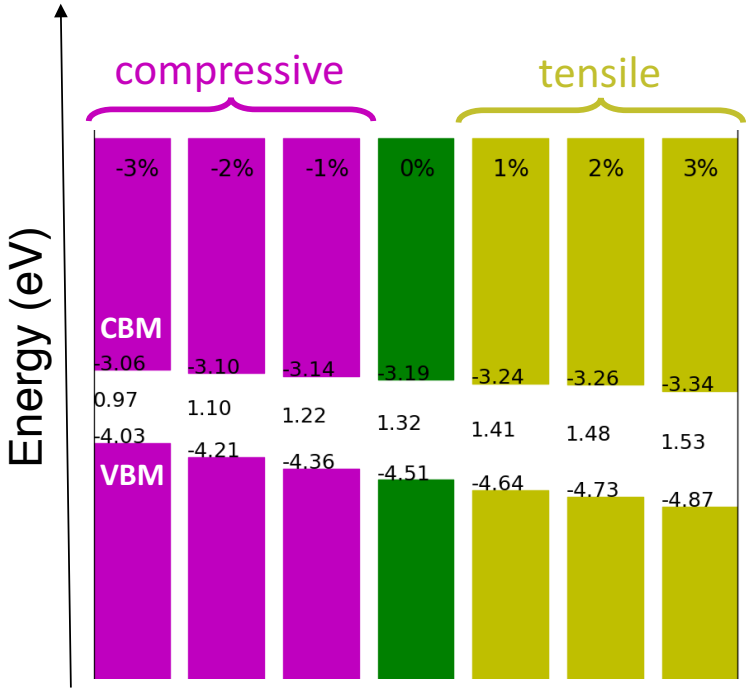

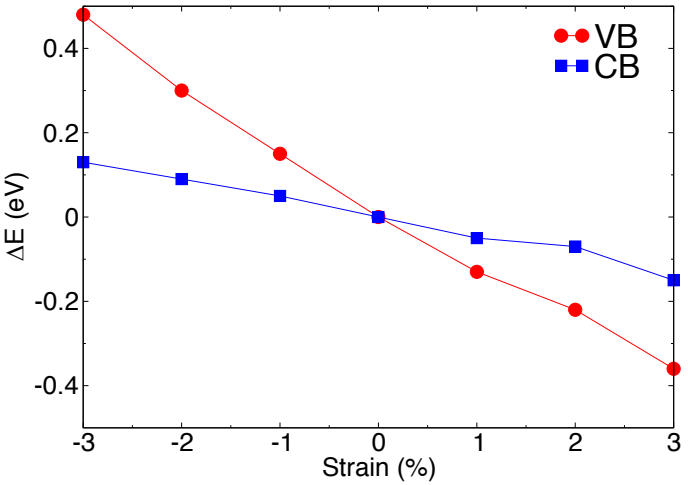

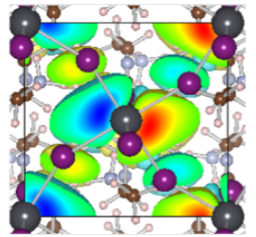

CBM_2[2]

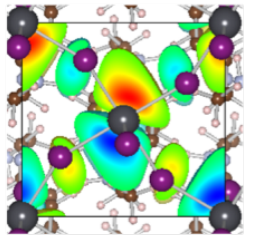

CBM_1[2]

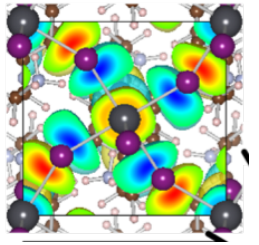

VBM[2]

Take home message

1. VBM downshift with tensile strain
2. VBM upward shift with compressive strain
3. CBM less affected

[1] B. Traore, to be published; [2] J. Even, PRB 86, 205301 (2012)

Results | theoretical framework relating microscopic surface and interface dipoles and work function(s)

method: DFT-1/2 + SOC

- two differently terminated surfaces of cubic $CsPbI_3$ slab
  - CsI and PbI_2-terminated surfaces

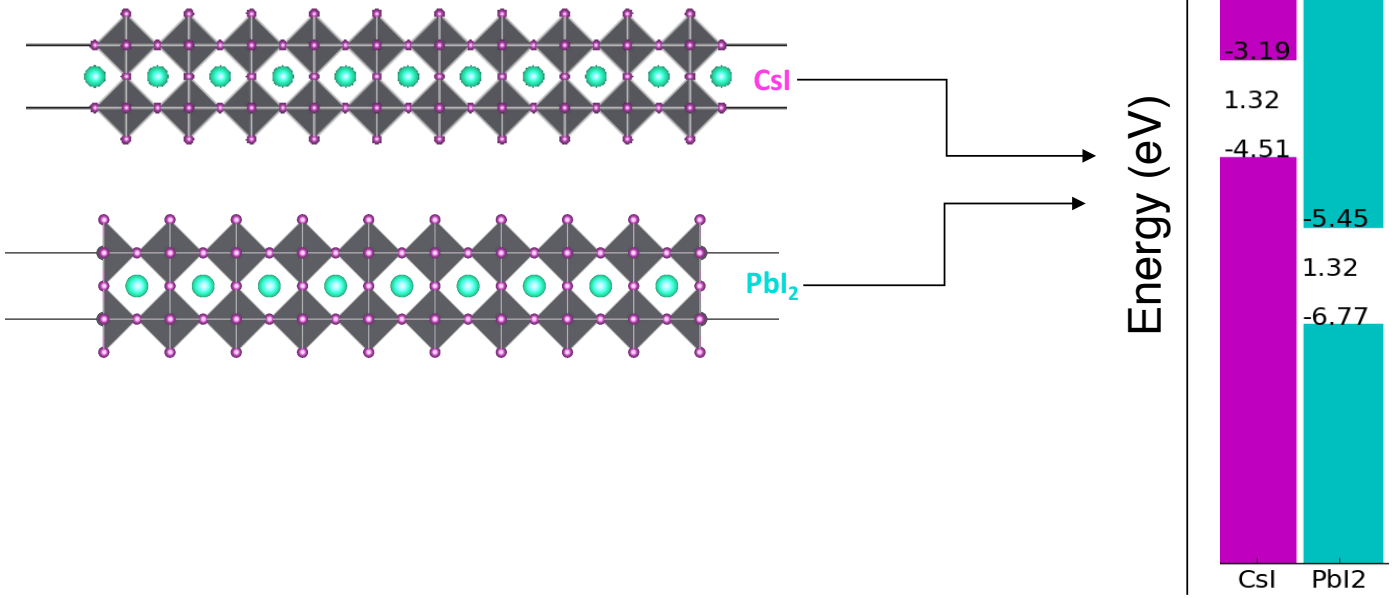

- The two surfaces result in very different absolute valence energy level alignments

How are these surface terminations' induced changes connected to surface dipoles?

[1] B. Traore, ACS Energy Lett., 7, 349 (2022);

Results | theoretical framework relating microscopic surface and interface dipoles and work function(s)

- empirical expression derived from Helmholtz equation[1]:

  potential drop

$$\Delta V = \frac{N\mu \cos\theta}{\varepsilon_r \varepsilon_0} \qquad \Delta\mathrm{WF} = -e\,\Delta V$$

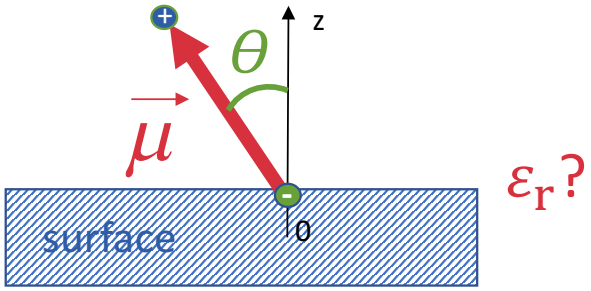

  - positive dipole WF decreases
  - negative dipole WF increases

[1] G. Ashkenasi, Acc. Chem. Res. 35, 121 (2002);

Results | theoretical framework relating microscopic surface and interface dipoles and work function(s)

- empirical expression derived from Helmholtz equation[1]:

  potential drop

$$\Delta V = \frac{N\mu \cos\theta}{\varepsilon_r \varepsilon_0} \qquad \Delta\mathrm{WF} = -e\,\Delta V$$

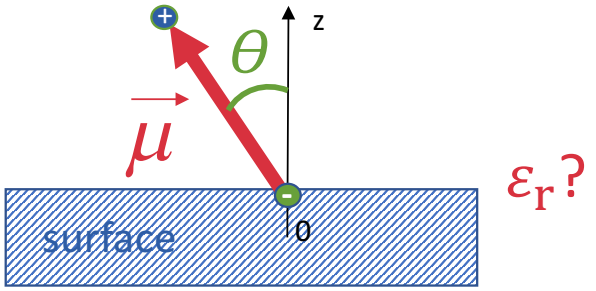

  - positive dipole WF decreases
  - negative dipole WF increases

- Leung et al.[2] use Poisson equation to link: $\Delta\mathrm{WF} \propto \Delta\mathrm{p}$

  $\Delta\mathrm{p}$ = change in surface dipole density

$$p = \int_{z_0}^{c/2} z\rho(z)dz$$

- perovskites: a posteriori correlations between $\Delta\mathrm{WF}$ and $\Delta\mathrm{p}$[3,4]
- Canil et al.[3]: SAMs tune perovskites energetics

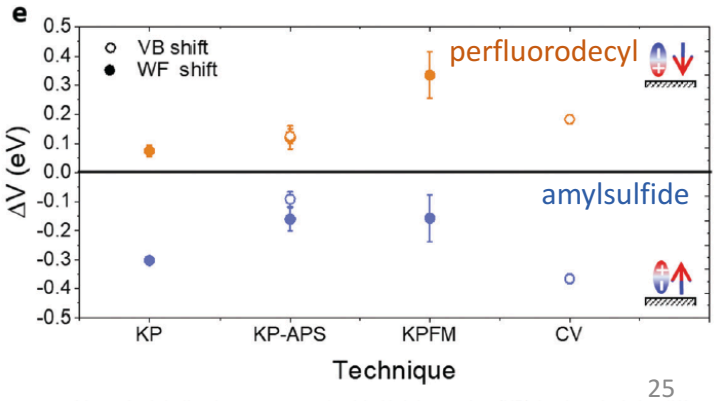

[1] G. Ashkenasi, Acc. Chem. Res. 35, 121 (2002); [2] T. C. Leung, PRB 68, 195408 (2003); [3] L. Canil, Energy Environ. Sci. 14, 1429 (2021); [4] ACS Energy Lett., 6, 2328 (2021); [5] G. Volonakis, J. Phys. Chem. Lett. 6, 2496(2015)

Results | theoretical framework relating microscopic surface and interface dipoles and work function(s)

- Computational methodology[1]:
  - Maxwell equation for insulators/dielectrics
  - planar averaged bound charge density $\rho(z) = -\frac{\partial P_z}{\partial z}$
  - planar average potential $V(z)$
  - dipole moment density and Poisson's equation $p = \int_{z_0}^{c/2} z\rho(z)dz = \int_{z_0}^{\frac{c}{2}} P_z(z)dz = -\varepsilon_0 \int_{z_0}^{\frac{c}{2}} dV(z)$

$$WF = eV\left(\frac{c}{2}\right) = eV(z_0) + \frac{e.p}{\varepsilon_0}$$

$$\Delta WF = \frac{e.\Delta p}{\varepsilon_0}$$

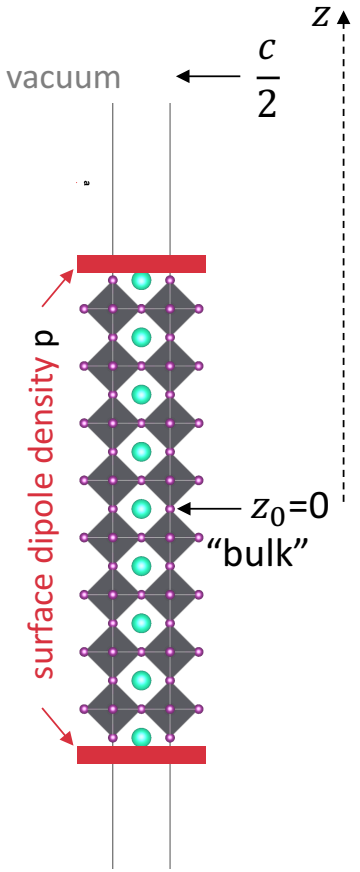

[1] B. Traore, ACS Energy Lett., 7, 349 (2022);

Results | theoretical framework relating microscopic surface and interface dipoles and work function(s)

- Computational methodology[1]:
  - Maxwell equation for insulators/dielectrics
  - planar averaged bound charge density $\rho(z) = -\frac{\partial P_z}{\partial z}$
  - planar average potential $V(z)$
  - dipole moment density and Poisson's equation $p = \int_{z_0}^{c/2} z\rho(z)dz = \int_{z_0}^{\frac{c}{2}} P_z(z)dz = -\varepsilon_0 \int_{z_0}^{\frac{c}{2}} dV(z)$

$$WF = eV\left(\frac{c}{2}\right) = eV(z_0) + \frac{e.p}{\varepsilon_0}$$

$$\boxed{\Delta WF = \frac{e.\Delta p}{\varepsilon_0}}$$

- recover Leung et al. (*sign*)[2]

$$\Delta V = \frac{N\mu \cos\theta}{\boldsymbol{\varepsilon_r}\varepsilon_0}$$

- further evaluation of the composite nature of the multi-layered perovskites
  - quantum confinement/type I band alignment[3,4]
  - dielectric confinement/electric susceptibility[4]

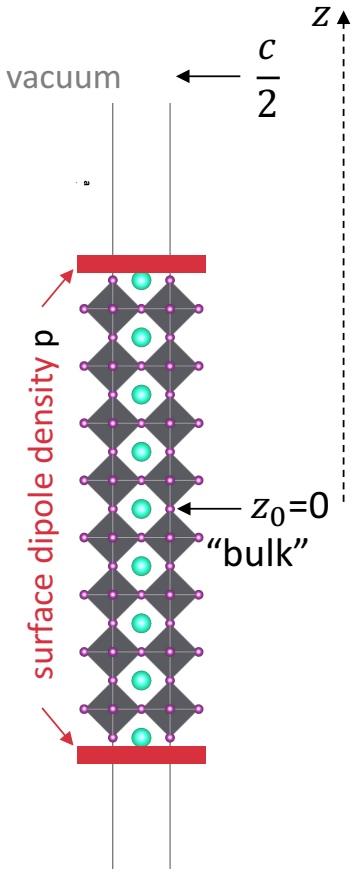

[1] B. Traore, ACS Energy Lett., 7, 349 (2022); [2] T. C. Leung, PRB 68, 195408 (2003); [3] J. Even, ChemPhysChem 15, 3733 (2014); [4]B. Traore, ACS Nano 12, 3321 (2018)

Results | Energetics of bare surfaces

CsI terminated

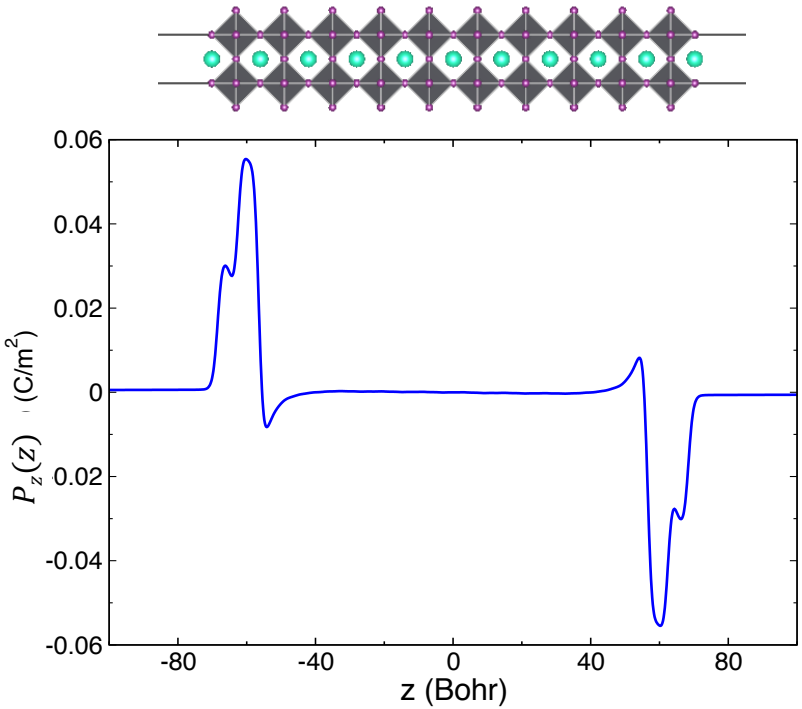

$$dipole\ density\ p = \int_{z_0}^{z} P_z(z)dz = 2.77\times10^{-11}\ C/m$$

[1] B. Traore, ACS Energy Lett., 7, 349 (2022);

Results | Energetics of bare surfaces

PbI_2 terminated

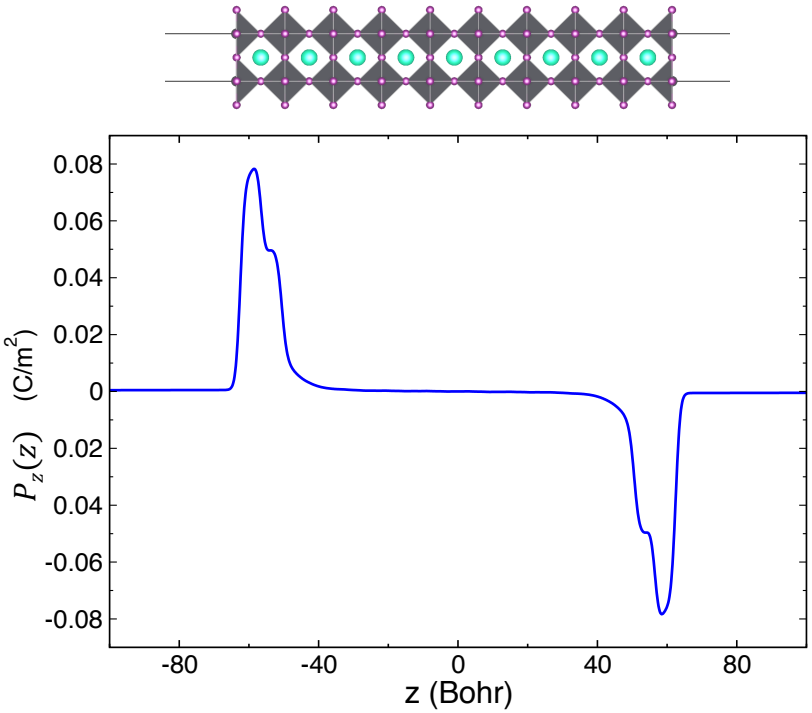

$$dipole\ density\ p = \int_{z_0}^{z} P_z(z)dz = 4.72\times10^{-11}\ C/m$$

[1] B. Traore, ACS Energy Lett., 7, 349 (2022);

Results | Energetics of bare surfaces

PbI_2 terminated

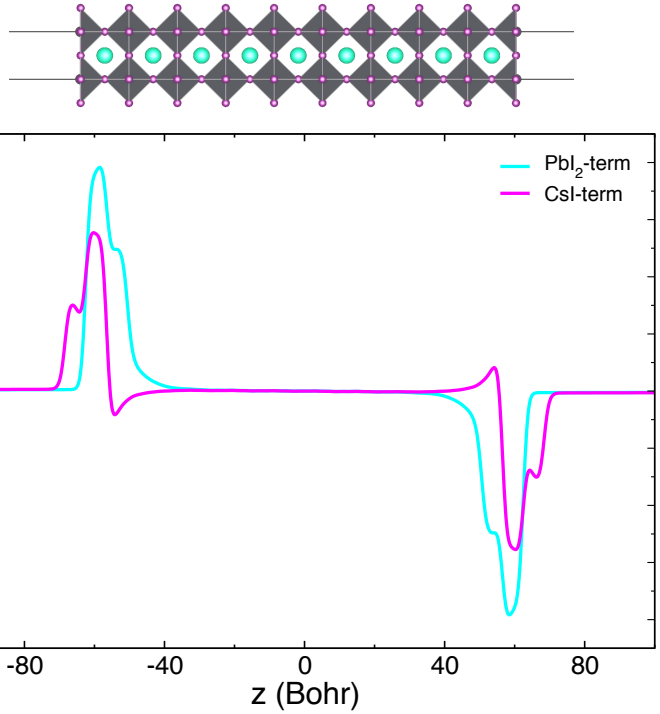

$$\Delta WF = \frac{e.\Delta p}{\varepsilon_0} = +2.27\ eV$$

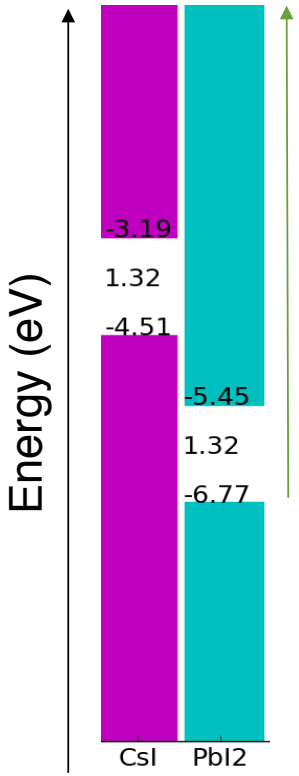

$$\Delta WF = -(E_v^{abs}(PbI_2) - E_v^{abs}(CsI))$$
$$= +2.26\ eV$$

WF increases

[1] B. Traore, ACS Energy Lett., 7, 349 (2022);

Results | Tuning Energetics with surface functionalization

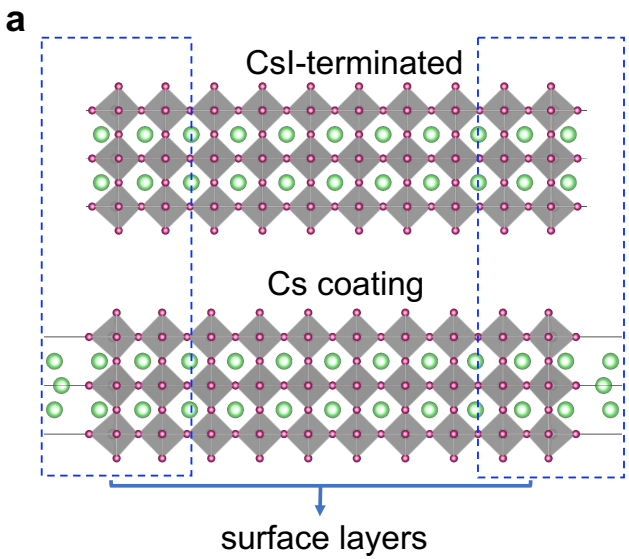

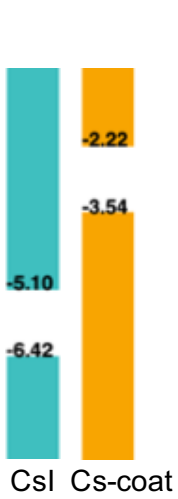

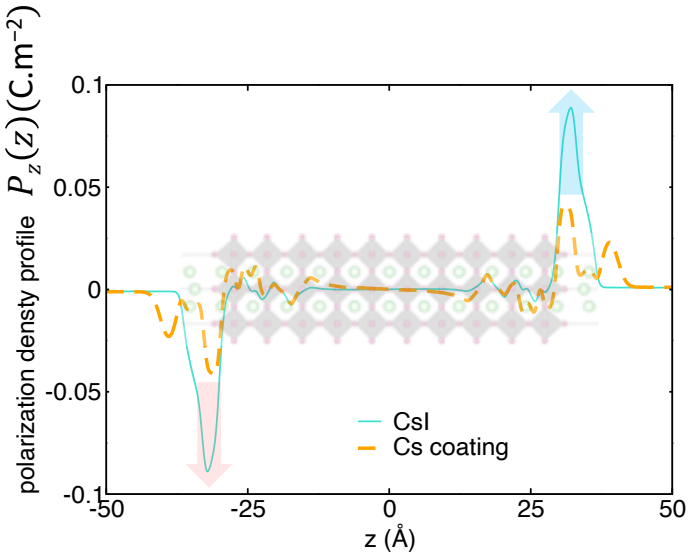

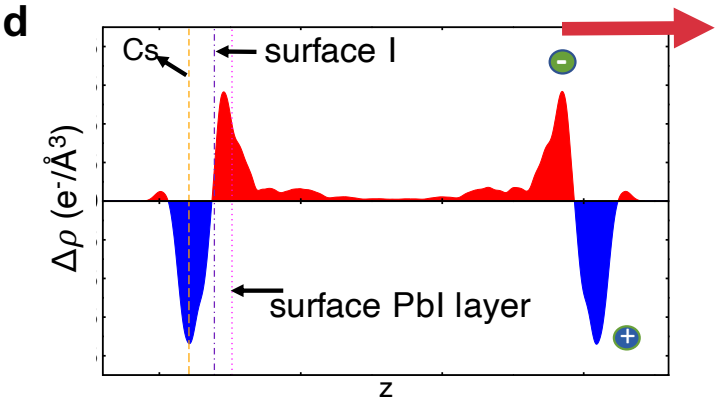

$$\Delta WF = -(E_v^{abs}(\text{Cs–coat}) - E_v^{abs}(\text{CsI})) = -2.88\ eV$$

$$\Delta WF = \frac{e.\Delta p}{\varepsilon_0} = -2.87\ eV$$

positive dipole: *WF* decreases, in line with lowering of the onset energy of the electron emission by ~ 2.2 eV[2]

[1] B. Traore, ACS Energy Lett., 7, 349 (2022); [2] F. Liu, Nat. Commun. 12, 673(2021)

Results | Connection to empirical potential drop

$CsPbBr_3$ slabs

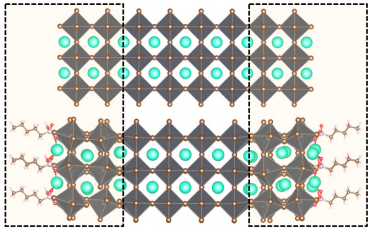

$$\Delta V = \frac{N\mu \cos\theta}{\varepsilon_r \varepsilon_0}$$

$$\Delta WF = -e\,\Delta V$$

DFT | empirical

ligand (25% coverage)	**ΔWF=** $-\Delta E_v^{abs}$	μ **(D)***	θ **(°)**	$\mu \cos\theta$ **(D)**	$\varepsilon_r = \frac{-e\,N\mu\cos\theta}{\varepsilon_0 \Delta WF}$		
Pentylphosphonic acid *phosphonate*	-0.30	1.40	4	1.40	1.28		
Pentanoic acid *oleate*	-0.45	1.59	11	1.56	0.95		
DMSO	-0.34	3.79	52	2.33	1.88		
Aniline	+0.36	1.70	167	-1.66	1.27		
p-methoxyaniline	+0.21	1.61	171	-1.59	2.08		
p-nitroaniline	+1.43	7.44	170	-7.33	1.41		

[1] P. Basera et al. unpublished;

Results | Connection to empirical potential drop

$$\Delta V = \frac{N\mu \cos\theta}{\varepsilon_r \varepsilon_0}$$

$$\Delta \mathrm{WF} = -e\,\Delta V$$

	DFT				empirical	DFT	
ligand (25% coverage)	**ΔWF=** $-\Delta E_v^{abs}$	μ **(D)***	θ **(°)**	$\mu \cos\theta$ **(D)**	$\varepsilon_r = \frac{-e\,N\mu\cos\theta}{\varepsilon_0 \Delta WF}$	ε_{r1}	ε_{r2}
Pentylphosphonic acid *phosphonate*	-0.30	1.40	4	1.40	1.28	4.7	1.19
Pentanoic acid *oleate*	-0.45	1.59	11	1.56	0.95	4.7	1.15
DMSO	-0.34	3.79	52	2.33	1.88	4.7	1.12
Aniline	+0.36	1.70	167	-1.66	1.27	4.7	1.23
p-methoxyaniline	+0.21	1.61	171	-1.59	2.08	4.7	1.28
p-nitroaniline	+1.43	7.44	170	-7.33	1.41	4.7	1.33

$CsPbBr_3$ slabs

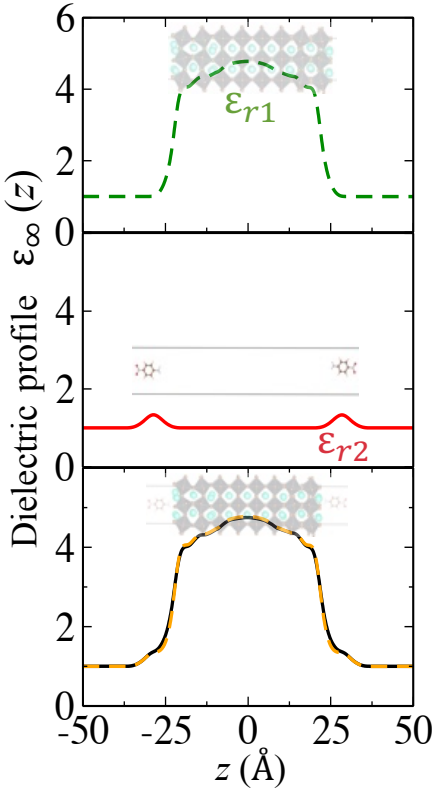

[1] P. Basera et al. unpublished; [2] B. Traore, ACS Nano 12, 3321 (2018)

Results | Heterostructure and additivity

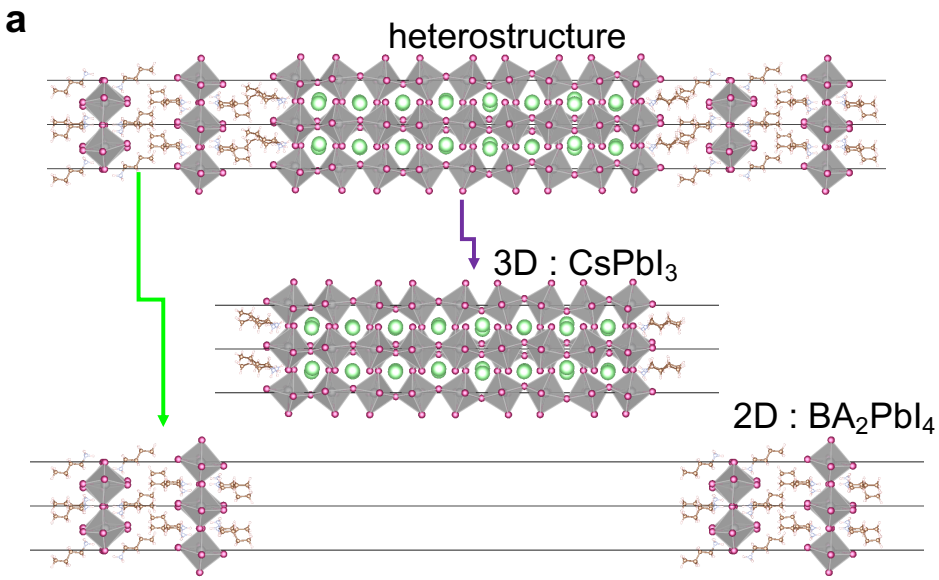

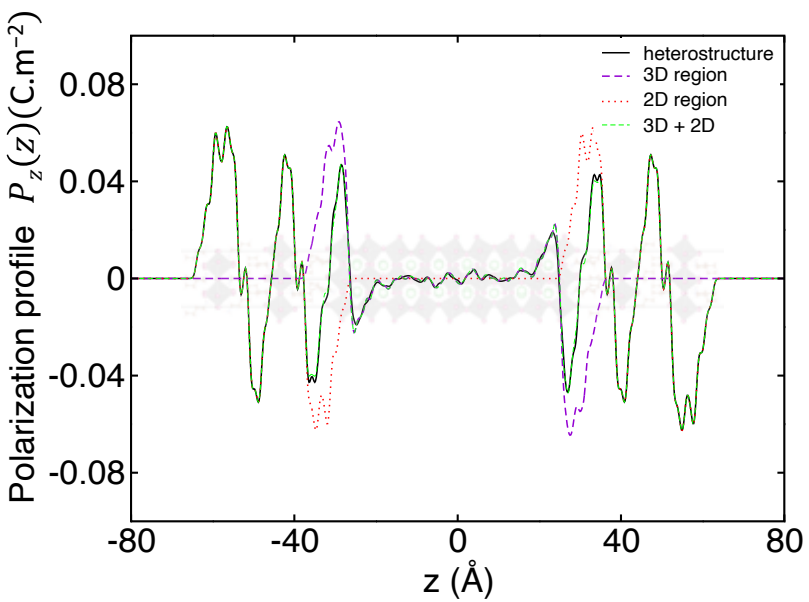

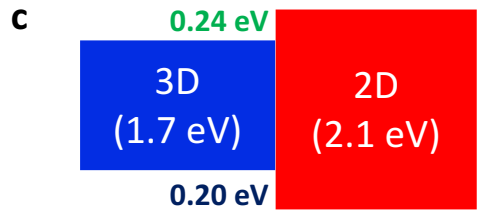

Take home message

1. microscopic understanding of WF shift
2. additivity of polarization profiles down to atomic scale
3. type I band alignment: barrier to both holes and electrons
4. *still challenging for 2D in large heterostructures (DFT-1/2)*

Conclusions | wrap up

Computational side

1. pseudo atom / VCA to mimic dynamic sisorder/alloying works
2. DFT-1/2 improves band gaps and effective masses
3. symmetry helps to tune relevant orbitals for 2D
4. xs-DFT-1/2 leads to an issue with absolute energetics
5. need for more experimental data on energetics and effective masses, especially for 2D
6. *organic still challenging*

strain and lattice mismatch

1. VBM downshift with tensile strain
2. VBM upward shift with compressive strain
3. CBM less affected
4. easily intuited from their orbital composition

Surface/Interface dipoles and energtics

1. microscopic understanding of WF shift
2. additivity of polarization profiles down to atomic scale
3. type I band alignment: barrier to both holes and electrons
4. *still challenging for 2D in large heterostructures (DFT-1/2)*

Conclusions | outlook

further optimization based on microscopic understanding of surface/interfaces

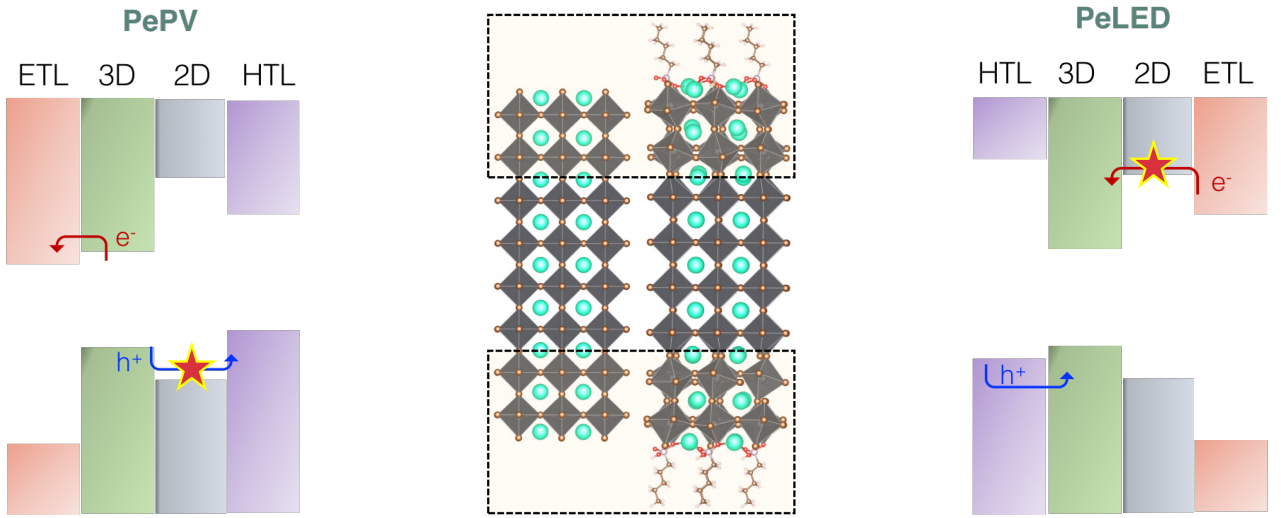

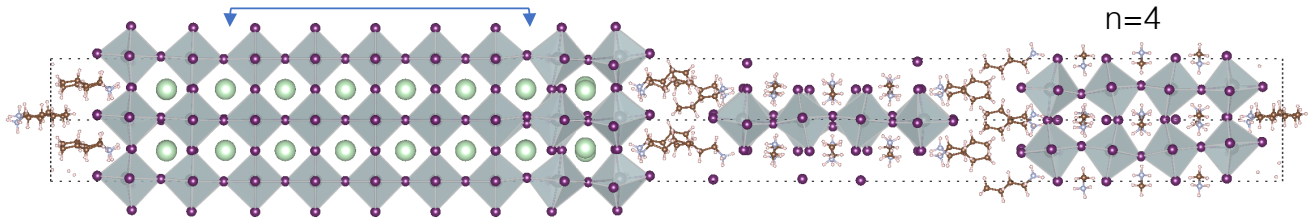

mixed halide mixed cation compositions $FA^{Cs}_{0.83}Cs^{Na}_{0.17}Pb(I_{0.83}Br_{0.17})_3$

Acknowledgments | perovskite team @rennes.fr

Acknowledgments

‘High-Performance Large Area Organic Perovskite devices for lighting, energy and Pervasive Communication’ (NMBP)

This project has received funding from the European Union’s Horizon 2020 research and innovation programme under grant agreement No 861985 (PeroCUBE).


HOPE FOR
PEACE

BONUS | DFT-1/2 for 3D

	Band gap (eV)		
	DFT	DFT-1/2	experiment
c-$FAPbI_3$	0.21	1.41	1.48 [1]
c-$CsPbI_3$	0.12	1.32	1.73 [2]
t-$CsPbI_3$	0.24	1.43	
o-$CsPbI_3$	0.51	1.66	
$CsPbBr_3$	0.69	2.16	2.25 [3]

	Band gap (eV)		
	DFT	DFT-1/2	experiment
RT-$MAPbI_3$	0.35	1.52	1.51 [4]
LT-$MAPbI_3$	0.55	1.69	1.65 [5]
$CsPbCl_3$	0.81	2.50	2.86 [6]
$FASnI_3$	0.00 (~no gap)	1.13	1.37 [7]

[1] Eperon *et al*, *Energy Environ Sc. 7*, 982, 2014
[2] Eperon *et al*, *J. Mater. Chem. A 3*, 19688, 2015
[3] Stoumpos et al., *Cryst. Growth Des.*, 13, 2722, 2013
[4] Shi et al., *Science* 347, 519, 2015
[5] Quarti et al., *Energy Environ Sc.* 9, 155, 2016
[6] Liu et al., *Proc. SPIE* 8852, 88520°, 2013
[7] Kahmann et al., *ACS Energy Lett.* 5, 2512, 2020

BONUS | Band gap of $Cs_xNa_{1-x}PbI_3$

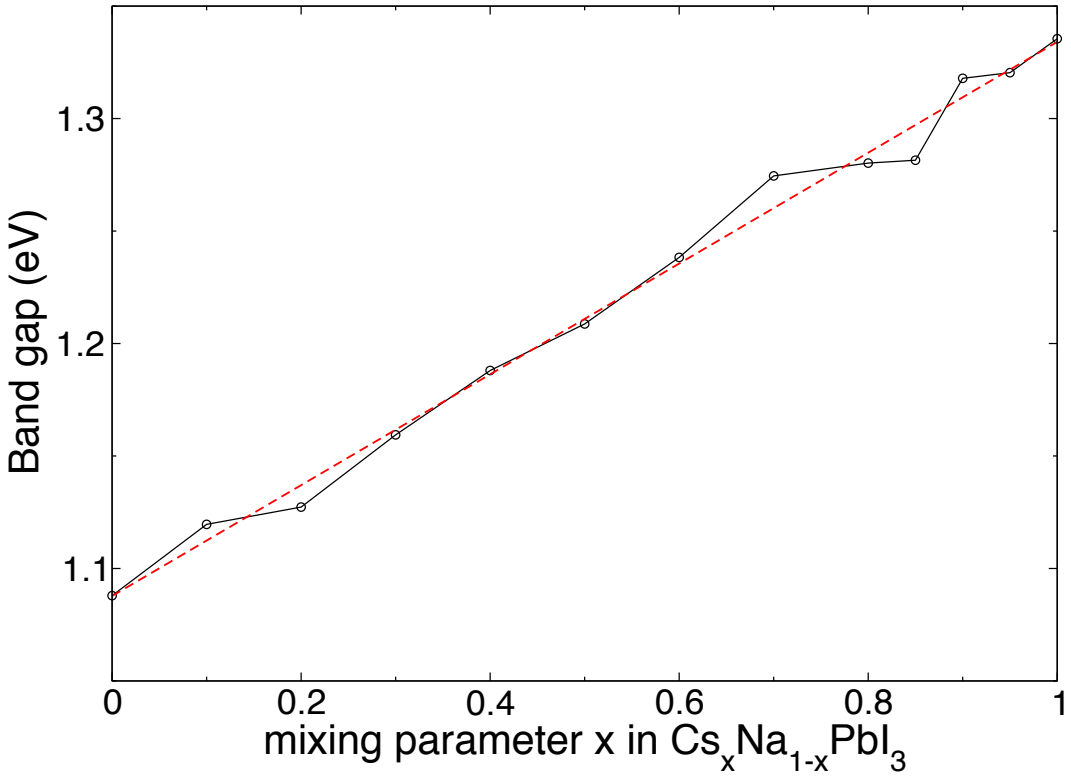

BONUS | Experimental Ionization energies of $MAPbI_3$

Selina Olthof

APL Mater. **4**, 091502 (2016)

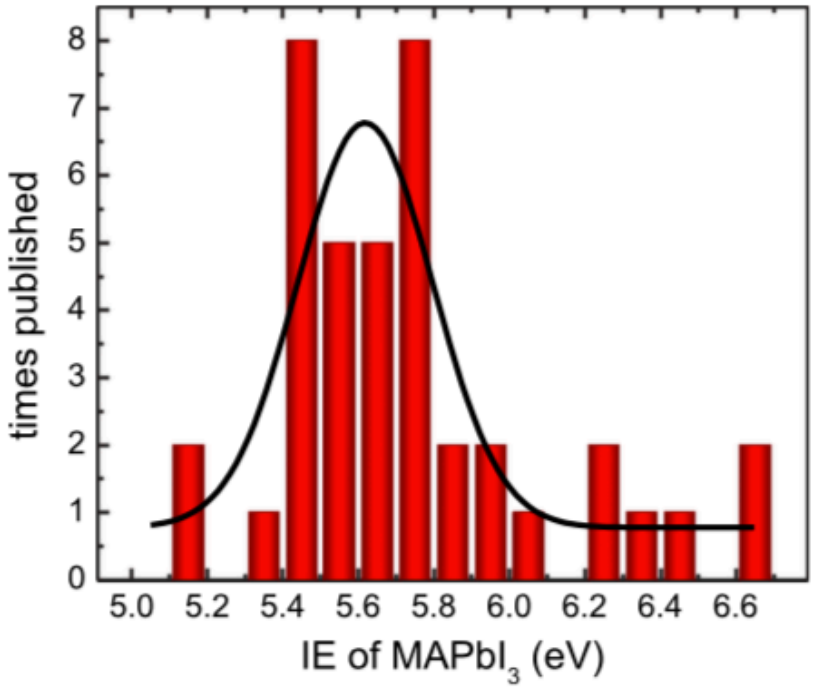

BONUS | Strain: epitaxial growth in semiconductors

coherent interfaces

expressions for (001) cubic phases

Tensile strain

$a_{L2} < a_{L1}$

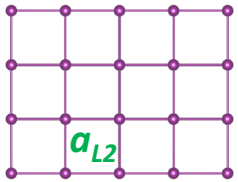

$\Delta < 0$

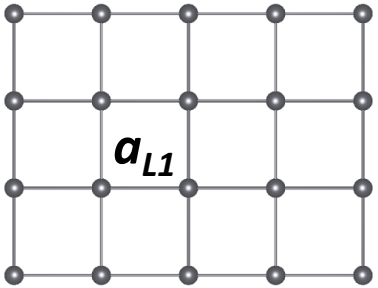

Lattice mismatch

$$\Delta = \frac{a_{L2} - a_{L1}}{a_{L2}}$$

$a_{L2} > a_{L1}$

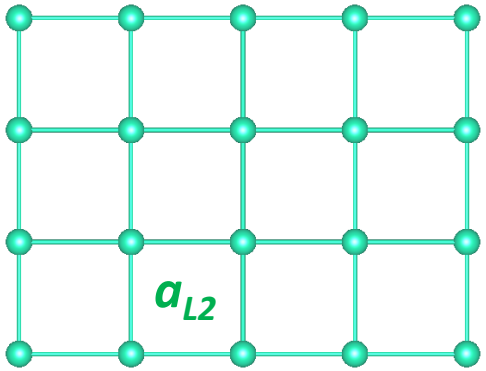

$\Delta > 0$

Compressive strain

elastic relaxation of the epitaxial layer

$$\varepsilon_{//} = \frac{a_{L1} - a_{L2}}{a_{L2}} = -\Delta$$

$$\varepsilon_{\perp} = \frac{-2C_{12}}{C_{11}} \varepsilon_{//}$$

$\varepsilon_{//} > 0$
$\varepsilon_{\perp} < 0$

$\varepsilon_{//} < 0$
$\varepsilon_{\perp} > 0$

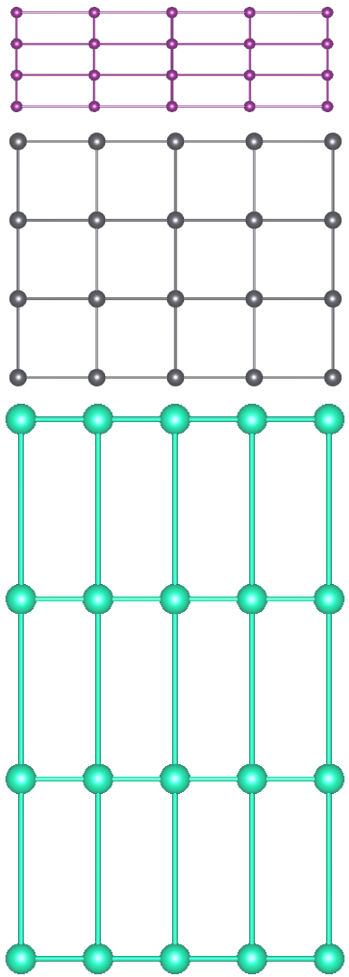

L1/L2 perovskite heterostructure

- *in-plane Surface the same for both*
- *different length along the stacking axis*
  l1= (n-1) c_{3D} and l2= c_{2D}
- *transverse elastic approximation*
- *free strain along the stacking axis*